Terrain Traversability Analysis using full-scale 3D Processing

Geert De Cubber and Haris Balta
Royal Military Academy of Belgium
Department of Mechanics, Unmanned Vehicle Centre
Avenue de la Renaissance 30, 1000 Brussels, Belgium
Email: geert.de.cubber@rma.ac.be; haris.balta@rma.ac.be

***Abstract*—Autonomous robotic systems which aspire to navigate through rough unstructured terrain require the capability to reason about the environmental characteristics of their environment. As a first priority, the robotic systems need to assess the degree of traversability of their immediate environment to ensure their mobility while navigating through these rough environments. This paper presents a novel terrain-traversability analyis methodology which is based on processing the full 3D model of the terrain, not on a projected or downscaled version of this model. The approach is validated using field tests using a time-of-flight camera.**

I. Introduction

More and more autonomous robotic systems are leaving the protected lab environment and entering the unstructured outside world. Applications like autonomous driving [1], demining [2], [3] and search and rescue [4] have already shown great promise for robots with autonomous capabilities. These autonomous robots generally rely on an advanced outdoor-capable navigation controller [5], [6] which is able to detect and negotiate driveable paths under multiple constraints. However, a major issue for the operation of such a navigation controller is that it requires information on the traversability of the terrain around the autonomous robot navigating through the environment.

A major problem for performing this terrain traversability analysis is that it requires an analysis of the 3D characteristics of the terrain in real-time. The advent of modern 3D sensing methodologies like RGB-D cameras, stereo vision systems and 3D laser scanners have made it now possible to acquire real-time 3D data, paving the way for performing on-line terrain traversability analysis based on that 3D data. In general, two types of approaches can be distinguished towards terrain traversability [7]:

- *Appearance-based* approaches employ image processing and classification algorithms to classify the terrain into several clusters (rocks, vegetation, road, gravel, etc). These approaches are particularly useful for planetary exploration robots [8], [9], as the type of objects to be encountered can (in general) quite well be predicted in advance. However, when confronted with natural environments, these approaches often have difficulties of correctly classifying the abundance of organic life forms (in particular: vegetation, trees, etc) under varrying athmospheric conditions.
- *Geometry-based* approaches build a terrain model and derive a set of corresponding features between data-point from the same class. Multi-scale processing (as also employed in the proposed approach) has already been introduced in the field of geometry-based terrain traversability approaches by Pai and Reissel in 1998 [10], which proposed an approach based on wavelet decomposition that modeled the terrain traversability in multiple resolution levels. Also the terrain traversability approach applied by Thrun et al. [11] on their robot that won the DARPA Grand Challenge falls into the category of geometry-based approaches. In this approach, a probabilistic framework was used to iteratively reduce the error on the traversability estimates.

The methodology presented in this paper falls into the category of geometry-based approaches as it is based on a reasoning process on a terrain model. However, traditional terrain traversability estimation algorithms [7] generally do not process the full 3D dataset (acquired via a 3D laser [12], a stereo camera [13], a time-of flight camera [14] or a combination of those [15]) in real-time, but concentrate on quickly downscaling (or projecting) the massive data-stream to a manageable size and performing an analysis in 2D or 2.5D.

The methodology presented here follows an inverse approach and aspires to perform a full-scale analysis on the measured 3D data from the terrain in front of the robot. The methodology is based on an analysis of the evolution of multi-scale normals evaluated at each data-point. The proposed methodology is validated using 3D data acquired by a 3D outdoor-capable time-of-flight camera mounted on an unmanned ground vehicle which is a validation platform for a search and rescue robot [16].

Results from this validation are presented in this article and show that the terrain traversability methodology successfully differentiates between non-surmountable obstacles and drivable terrain. However, due to the required processing power for the proposed methodology, it is (at present) not yet possible to perform all required calculations in real-time. The use of the methodology is therefore for the moment still restricted to off-line usage, until the embedded computing capabilities increase.

Fig. 1. Image of the example frame being processed

II. Proposed Methodology

The proposed methodology builds upon our earlier work on terrain traversability analysis and is based upon the analysis of multi-scale normals. To explain the methodology, the algorithm is explained here, visually showing the result of each processing step, starting from a baseline frame as shown in Figure 1. The dataset which was used for this validation process consists of a 3D image sequence acquired by a PMD CamCube time-of-flight camera, embedded on a search and rescue robot [16].

The sole input to the algorithm is considered to be an $m \times n$ 3D point cloud $\boldsymbol{x}$, which can consist (depending on the type of acquisition device) of millions of 3D points.

The first step of the algorithm consists of searching for each 3D data point $\boldsymbol{x}_i$ the corresponding points $\boldsymbol{x}_j$, such that:

$$\parallel \boldsymbol{x}_i - \boldsymbol{x}_j \parallel^2 \leq r_k \tag{1}$$

where r_k is a multi-scale radius, defined as:

$$r = \frac{2^c}{\sqrt{m.n}} \tag{2}$$

with c being the considered radius or scale.

In a following step, the vector normals $\boldsymbol{v}_i^c$ to the N points in the $\boldsymbol{x}_j$ point cloud are calculated.

Up until this step, we have selected the data points which are within a certain radius from the base point and we have calculated the different normals from each of these points. The main idea behind the proposed traversability estimation methodology is now that in the presence of non-traversable terrain or obstacles, these normals will point in different directions, whereas driveable terrain should be characterized by a lower level of variation among the normals.

As such, a first-order traversability score can be determined by calculating the vector variation on the data normals as follows:

$$\boldsymbol{\tau}_i^c = \sqrt{\frac{\sum_{k=1}^{N} (\boldsymbol{v}_i^c(k) - \overline{\boldsymbol{v}_i^c})^2}{N}} \tag{3}$$

Note that the traversbility score is thus evaluated for each separate data point i and is also dependent on the radius or scale, expressed by the parameter c.

Figure 2 shows the result of applying the proposed traversability scoring methodology over the different radii. Note that the traversability maps in Figure 2 are in fact full 3D maps, but for reasons of clarity, only top-down views are presented.

When analysing Figure 2, the effect of applying the multi-scale approach, selecting different radii for calculating the vector variation of the normals, becomes apparent.

- Using small radii ($c \leq 3$), only few data points are selected for calculating the variation of the normals, meaning that the signal-to-noise ration is too low to draw conclusions.
- Using small radii ($c \geq 8$), too much data points are selected for calculating the variation of the normals, meaning that one is more calculating a mean vector variation over the whole field and it is not possible to draw conclusions on local features.

From Figure 2, it is evident that the optimal scale or radius for being able to draw conclusions on the traversability of the terrain is clearly between 5 and 7.

At this point, we assume that the majority of the terrain is traversable. While it is true that this is an assumption which may not always hold, it must not be forgotten that we have so far only considered one single frame. In an on-line traversability estimation context, the algorithm would iteratively estimate successive frames, accummulating the data over the different frames. In such a context, it could be safely assumed that the majority of the terrain visible in only the very first frame corresponds to traversable terrain, whereas this assumption does not need to be necessarily extended to all acquired frames.

Under this assumption, the traversability can be further refined by comparing the traversability score at a very high radius (which should correspond to the traversability score for the traversable terrain) with the traversability score at a medium level, e.g.:

$$\boldsymbol{\tau}_i = \parallel \boldsymbol{\tau}_i^6 - \boldsymbol{\tau}_i^{12} \parallel \tag{4}$$

These $\boldsymbol{\tau}_i$ still represent a 3-vector for each data point, which is undesired. In order to define a single final traversability score per data point, the standard deviation over this vector is applied as follows:

$$\tau_i = \sqrt{\frac{\sum_{k=1}^{3} (\boldsymbol{\tau}_i(k) - \overline{\boldsymbol{\tau}_i})^2}{3}} \tag{5}$$

with τ_i being the final traversability score per data point i.

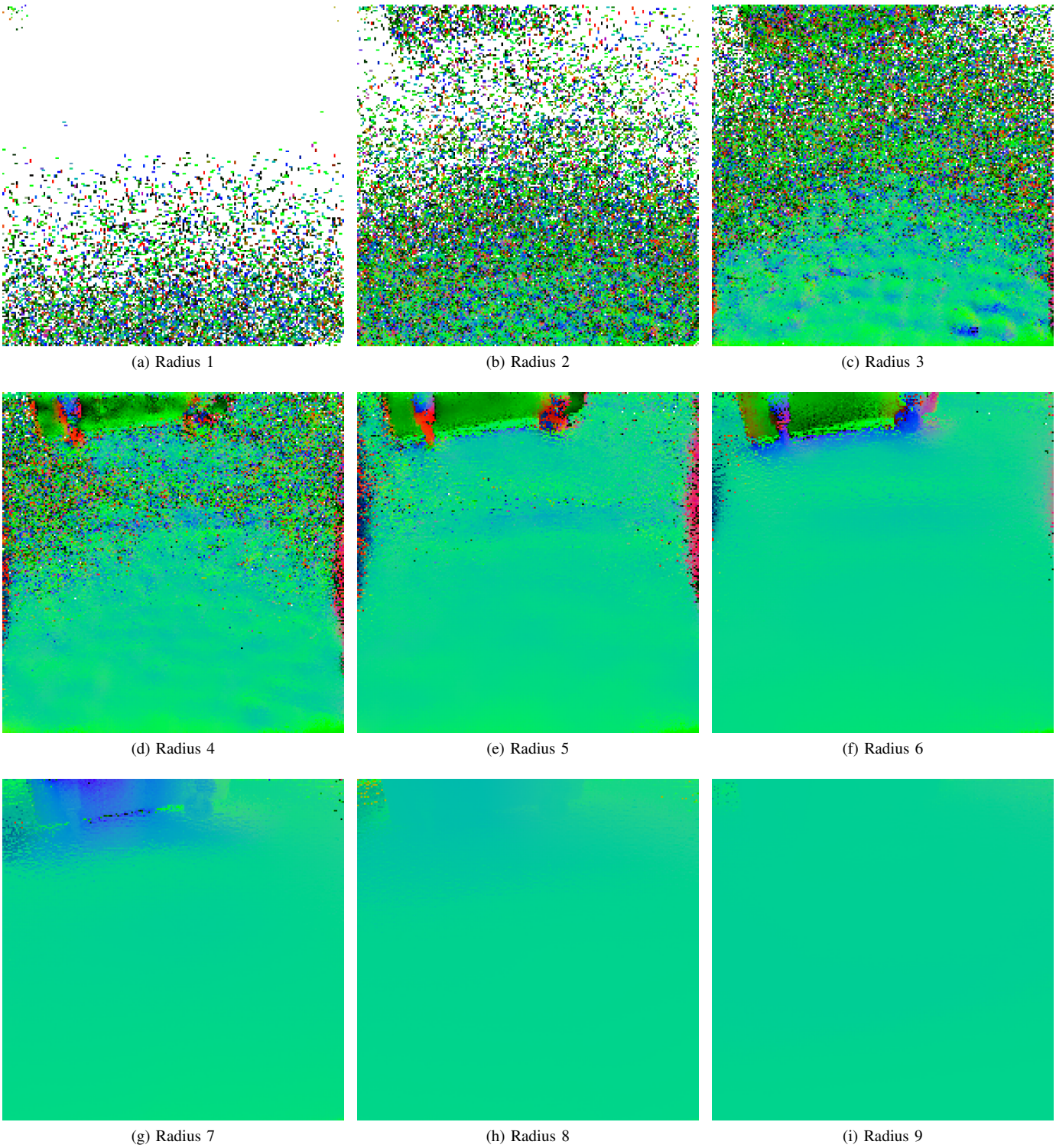

(a) Radius 1 (b) Radius 2 (c) Radius 3

(d) Radius 4 (e) Radius 5 (f) Radius 6

(g) Radius 7 (h) Radius 8 (i) Radius 9

Fig. 2. Vector variation of the multi-scale normals. The colors of the images represent the orientation of the multi-scale normals $\boldsymbol{\tau}_i^c$

III. Results and Validation

Figure 3 shows the final result of the proposed terrain traversability estimation approach as a projected 2D map. Note how the container object on the top left of the image can be clearly distinguished. Figure 3 also shows that the methodology does have as a disadvantage that - for the moment - it does not include a methodology to exclude shadowing effects due to the measurement principle of the time-of-flight camera. This was partly done on purpose, as we wanted to develop a methodology which would be agnostic towards the type of sensor (Laser, stereo camera, time-of-flight camera, kinect-type of camera, etc). The result of this is that the shadow

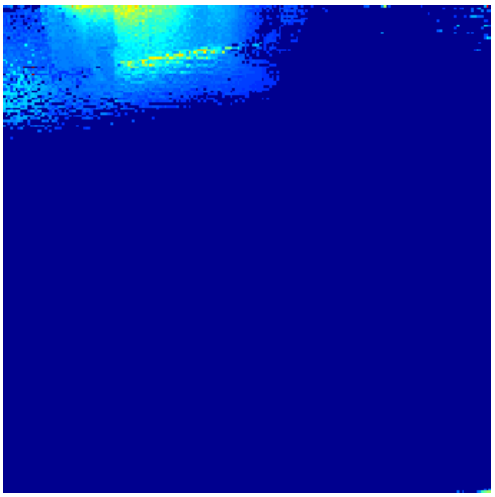

Fig. 3. 2D Result of the proposed terrain traversability approach

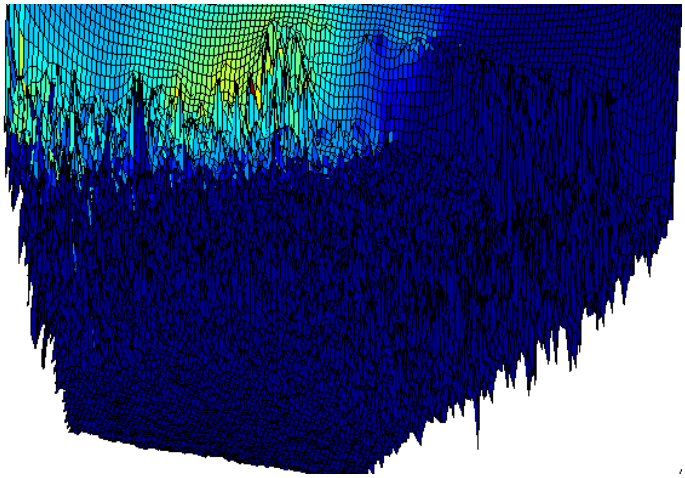

Fig. 4. 3D Result of the proposed terrain traversability approach

of the container on the top left is also (wrongly) classified as an obstacle. Aside from this effect, there are very few wrong classifications. Only in the top right corners, some false positives are visible, which are due to the very low signal-to-noise ration at larger distances, close to the maximum viewing distance of 7.5 meters of the PMD time-of-flight sensor.

Figure 4 shows the same result as Figure 3, but this time in a 3D view. While the 3D view is herder to interprete on a 2D interface, it also shows clearly the detected obstacle on the far left side, while the rest of the terrain is correctly classified as traversable (blue).

IV. Conclusion

In this paper, we have introduced a novel methodology for terrain traversability analysis by analyzing the full 3D signal of a 3D acquisition device. The methodology is based on the analysis of multi-resolution normals, selecting the optimal resolution to perform the classification of the terrain. While this methodology it is still too slow to be used on-line using present-day embedded computing infrastructure, the results are promising, which opens the door for implementation on future robotic systems which need to navigate on rough terrain.

Acknowledgment

The research leading to these results has received funding from the European Communitys Seventh Framework Programme (FP7/2007-2013) under grant agreement number 285417.

References

[1] A. Broggi, S. Debattisti, P. Grisleri, M. C. Laghi, P. Medici, and P. Versari, "Extensive Tests of Autonomous Driving Technologies," *IEEE Trans. on Intelligent Transportation Systems*, vol. 14, no. 3, pp. 1403–1415, Sep. 2013, iSSN: 1524-9050.

[2] Y. Yvinec, Y. Baudoin, G. De Cubber, M. Armada, L. Marques, J.-M. Desaulniers, and M. Bajic, "Tiramisu : Fp7-project for an integrated toolbox in humanitarian demining," in *GICHD Technology Workshop*, 2012.

[3] E. Colon, G. De Cubber, H. Ping, J.-C. Habumuremyi, H. Sahli, and Y. Baudoin, "Integrated robotic systems for humanitarian demining," *International Journal of Advanced Robotic Systems*, vol. 4, no. 2, pp. 219–228, Jun. 2007.

[4] G. De Cubber, D. Doroftei, D. Serrano, K. Chintamani, R. Sabino, and S. Ourevitch, "The eu-icarus project: developing assistive robotic tools for search and rescue operations," in *Safety, Security, and Rescue Robotics (SSRR), 2013 IEEE International Symposium on*. IEEE, 2013, pp. 1–4.

[5] C. Armbrust, G. De Cubber, and K. Berns, "ICARUS - control systems for search and rescue robots," *Field and Assistive Robotics: Advances in Systems and Algorithms*, vol. 1, pp. 1–16, May 2014.

[6] D. Doroftei, G. De Cubber, E. Colon, and Y. Baudoin, "Behavior based control for an outdoor crisis management robot," in *Proceedings of the IARP International Workshop on Robotics for Risky Interventions and Environmental Surveillance*, 2009, pp. 12–14.

[7] P. Papadakis, "Terrain traversability analysis methods for unmanned ground vehicles: A survey," *Engineering Applications of Artificial Intelligence*, vol. 26, no. 4, pp. 1373 – 1385, 2013.

[8] A. Howard, H. Seraji, and E. Tunstel, "A rule-based fuzzy traversability index for mobile robot navigation," in *In: IEEE Intl. Conf. Robotics and Automation. Seoul, Korea*, 2001, pp. 3067–3071.

[9] A. Howard and H. Seraji, "Vision-based terrain characterization and traversability assessment," *Journal of Robotic Systems*, vol. 18, no. 10, pp. 577–587, 2001.

[10] D. K. Pai and L. Reissell, "Multiresolution rough terrain motion planning," *IEEE T. Robotics and Automation*, vol. 14, no. 1, pp. 19–33, 1998.

[11] S. Thrun, M. Montemerlo, H. Dahlkamp, D. Stavens, A. Aron, J. Diebel, P. Fong, J. Gale, M. Halpenny, K. Lau, C. Oakley, M. Palatucci, V. Pratt, P. Stang, S. Strohb, C. Dupont, L. erik Jendrossek, C. Koelen, C. Markey, C. Rummel, J. V. Niekerk, E. Jensen, G. Bradski, B. Davies, S. Ettinger, A. Kaehler, A. Nefian, and P. Mahoney, "The robot that won the darpa grand challenge," *Journal of Field Robotics*, vol. 23, pp. 661–692, 2006.

[12] F. Neuhaus, D. Dillenberger, J. Pellenz, and D. Paulus, "Terrain drivability analysis in 3d laser range data for autonomous robot navigation in unstructured environments," in *Emerging Technologies Factory Automation, 2009. ETFA 2009. IEEE Conference on*, Sept 2009, pp. 1–4.

[13] G. De Cubber, D. Doroftei, L. Nalpantidis, G. C. Sirakoulis, and A. Gasteratos, "Stereo-based terrain traversability analysis for robot navigation," in *IARP/EURON Workshop on Robotics for Risky Interventions and Environmental Surveillance*, Brussels, Belgium, 2009.

[14] G. De Cubber, D. Doroftei, H. Sahli, and Y. Baudoin, "Outdoor terrain traversability analysis for robot navigation using a time-of-flight camera," in *RGB-D Workshop on 3D Perception in Robotics*, 2011.

[15] G. De Cubber and D. Doroftei, "Multimodal terrain analysis for an all-terrain crisis management robot," in *IARP HUDEM 2011*, 2011.

[16] H. Balta, G. De Cubber, D. Doroftei, Y. Baudoin, and H. Sahli, "Terrain traversability analysis for off–road robots using time-of-flight 3d sensing," in *7th IARP International Workshop on Robotics for Risky Environment-Extreme Robotics*, Saint-Petersburg, Russia, 2013.